

# MAIN RESULTS OF THE FIRST EXPERIMENTAL CAMPAIGN IN THE STELLARATOR W7-X

N.B. Marushchenko<sup>1</sup>, A. Dinklage<sup>1</sup>, A. Alonso<sup>2</sup>, J. Baldzuhn<sup>1</sup>, C.D. Beidler<sup>1</sup>,  
C. Biedermann<sup>1</sup>, B. Blackwell<sup>3</sup>, S. Bozhenkov<sup>1</sup>, R. Brakel<sup>1</sup>, B. Buttenschön<sup>1</sup>, Y. Feng<sup>1</sup>,  
G. Fuchert<sup>1</sup>, J. Geiger<sup>1</sup>, M. Hirsch<sup>1</sup>, U. Hoefel<sup>1</sup>, J. Knauer<sup>1</sup>, A. Krümer-Flecken<sup>4</sup>,  
A. Langenberg<sup>1</sup>, H.P. Laqua<sup>1</sup>, M. Landreman<sup>5</sup>, H. Maassberg<sup>1</sup>, N.A. Pablant<sup>6</sup>, E. Pasch<sup>1</sup>,  
K. Rahbarnia<sup>1</sup>, L. Rudischhauser<sup>1</sup>, T. Stange<sup>1</sup>, L. Stephey<sup>7</sup>, H. Trimino-Mora<sup>1</sup>, Yu. Turkin<sup>1</sup>,  
J.-L. Velasco<sup>2</sup>, G. Wurden<sup>8</sup>, D. Zhang<sup>1</sup>, T. Andreeva<sup>1</sup>, M. Beurskens<sup>1</sup>, E. Blanco<sup>2</sup>,  
H.-S. Bosch<sup>1</sup>, R. Burhenn<sup>1</sup>, A. Cappa<sup>2</sup>, A. Czarnecka<sup>9</sup>, M. Dostal<sup>4</sup>, P. Drews<sup>4</sup>, M. Endler<sup>1</sup>,  
T. Estrada<sup>2</sup>, T. Fornal<sup>9</sup>, O. Grulke<sup>1</sup>, D. Hartmann<sup>1</sup>, J.H. Harris<sup>10</sup>, P. Helander<sup>1</sup>,  
M. Jakubowski<sup>1</sup>, T. Klinger<sup>1</sup>, S. Klose<sup>1</sup>, G. Kocsis<sup>11</sup>, R. König<sup>1</sup>, P. Kornejew<sup>1</sup>, N. Krawczyk<sup>9</sup>,  
M. Krychowiak<sup>1</sup>, M. Kubkowska<sup>9</sup>, I. Kiazek<sup>12</sup>, S. Lazerson<sup>6</sup>, Y. Liang<sup>4</sup>, S. Liu<sup>4</sup>, O. Marchuk<sup>4</sup>,  
S. Marsen<sup>1</sup>, V. Moncada<sup>13</sup>, D. Moseev<sup>1</sup>, D. Naujoks<sup>1</sup>, H. Niemann<sup>1</sup>, M. Otte<sup>1</sup>, T.S. Pedersen<sup>1</sup>,  
F. Pisano<sup>14</sup>, K. Riße<sup>1</sup>, T. Rummel<sup>1</sup>, O. Schmitz<sup>7</sup>, S. Satake<sup>15</sup>, H. Smith<sup>1</sup>, T. Schröder<sup>1</sup>,  
T. Szepesi<sup>12</sup>, H. Thomsen<sup>1</sup>, P. Traverso<sup>16</sup>, M. Tsuchiya<sup>15</sup>, N. Wang<sup>4</sup>, T. Wauters<sup>17</sup>, G. Weir<sup>1</sup>,  
R. Wolf<sup>1</sup>, M. Yokoyama<sup>15</sup> and the W7-X Team

<sup>1</sup>Max Planck Institute for Plasma Physics, EUROATOM-Association, Greifswald, Germany;

<sup>2</sup>Laboratorio Nacional de Fusión, CIEMAT, Avenida Complutense, Madrid, Spain;

<sup>3</sup>Australian National University, Acton ACT, Canberra, Australia;

<sup>4</sup>Forschungszentrum Jülich GmbH, Institut für Energie- und Klimaforschung-Plasmaphysik,  
Partner of the Trilateral Euregio Cluster (TEC), Jülich, Germany;

<sup>5</sup>University of Maryland, College Park, MD, USA;

<sup>6</sup>Princeton Plasma Physics Laboratory, Princeton, New Jersey, USA;

<sup>7</sup>University of Wisconsin, Engineering Drive, Madison, Wisconsin, USA;

<sup>8</sup>Los Alamos National Laboratory, Los Alamos, New Mexico, USA;

<sup>9</sup>Institute of Plasma Physics and Laser Microfusion, Warsaw, Poland;

<sup>10</sup>Oak Ridge National Laboratory, Oak Ridge, Tennessee, USA;

<sup>11</sup>Wigner Research Centre for Physics, Konkoly Thege, Budapest, Hungary;

<sup>12</sup>Opole University, Opole, Poland;

<sup>13</sup>IRFM, CEA-Cadarache, France;

<sup>14</sup>Cagliari University, Cagliari, Italy;

<sup>15</sup>National Institute for Fusion Science, Toki, Japan;

<sup>16</sup>Auburn University, Auburn, USA;

<sup>17</sup>Laboratory for Plasmaphysics, LPP-ERM/KMS, Brussels, Belgium, TEC Partner

*E-mail: nikolai.marushchenko@ipp.mpg.de*

A summary of the first operational phase (OP1.1) at the stellarator W7-X is given. The operational setup of heating and diagnostics as well the results of experiments are briefly described. Plasma parameters and confinement are better than expected:  $T_e > 8$  keV and  $T_i > 2$  keV at  $\bar{n}_e \approx 3 \times 10^{19} \text{ m}^{-3}$  yielding  $\beta_0 \approx 2.5$  %. The results for ECR heating with X2-mode as well the ECCD are in good agreement with the theory predictions. The heating scenario with the O2-mode alone was successfully first time performed. Stellarator specific regime of core “electron root” confinement was obtained.

PACS: 28.52.-s, 52.25.-b, 52.25.Xz, 52.25.Os, 52.50.-b, 52.55.-s

## INTRODUCTION

In December, 10th, 2015, after approximately fifteen years of construction and one year commissioning, the stellarator Wendelstein 7-X (W7-X) began its work [1]. The path to this event includes the years of intensive investigations and use (or further develop) most advanced numerical tools on plasma physics, design engineering, metrology, tooling, and manufacturing —

everything to deal with fully 3D geometry. The 50 modular non-planar and the 20 planar super-conducting NbTi coils are the key components for the steady-state operation of the device. Manufacturing, test and assembly of the coils took in total eight years and considerable efforts were necessary due to extremely high quality and reliability requirements [2].

W7-X is the international project and starting from the first operational phase OP1.1 there is a strong

participation by the international partners from EU, USA, Japan and Australia.

W7-X, the modular stellarator equipped by superconducting coils [3, 4], belongs to the HELIAS line (HELICAL axis Advanced Stellarator) proposed by Nührenberg and Zille [5, 6]. W7-X is optimized with respect to good MHD stability for  $\beta < 5\%$ , improved neoclassical confinement, good confinement of fast particles, and low bootstrap current; see [4] and the references therein. A 3D shaping of the magnetic configuration gives an additional flexibility for an operation [7].

With a major radius,  $R_0$ , of 5.5 m and an average minor radius,  $\langle a \rangle$ , of 0.5 m the resulting plasma volume of  $30 \text{ m}^3$  lies between those of ASDEX Upgrade and JET. The maximum magnetic field is 3 T, corresponding to 600 MJ of magnetic field energy. The rotational transform,  $\iota$ , ranges from  $5/6$  to  $5/4$  and, in contrast to the partially optimized predecessor of W7-X, Wendelstein 7-AS (W7-AS) [8], is practically independent of plasma  $\beta$ .

The near-term focus is the scientific exploitation of the W7-X experiment in order to assess stellarator optimization in view of economic operation of a stellarator fusion power plant [9]. The high-level scientific goals of W7-X are the demonstration of improved neoclassical confinement as well as improved confinement of fast ions, further, plasma stability up to a volume-averaged  $\beta$  of 5%, and a stiff magnetic equilibrium to facilitate the island divertor concept [10] while achieving steady-state operation.

## 1. EXPERIMENTAL SETUP FOR OP1.1

For OP1.1, only electron-cyclotron-resonance heating (ECRH) was foreseen. Six from ten gyrotrons with power up to 1.0 MW each and a quasi-optical transmission line [11] have been applied for plasma start-up, heating and wall conditioning with a very high reliability. Frequency of gyrotrons 140 GHz corresponds to the cyclotron resonance at the 2nd harmonics for  $B_0 = 2.5 \text{ T}$ , and polarization of each RF beams can be chosen arbitrary, ordinary (O) or extraordinary (X) wave-mode.

One from the most definitive points for OP1.1 was that the five graphite claddings foreseen by design of divertor [12] were not installed (the latter is planned to be ready for the next campaigns) and, for example, the CuCrZr cooling structures of the heat shields had been uncovered. In order to solve it, five graphite limiters are installed at the torus inboard side [13]; (Fig. 1). Magnetic configuration for operation was modified in such a way that the magnetic surface which crosses the limiter was in outer vicinity of the island chain  $\iota = 5/6$ . So far, the effective radius of last magnetic surface was reduced to  $a = 0.49 \text{ m}$  and the work volume of plasmas to about  $26 \text{ m}^3$ . Since no active cooling down for the limiter was foreseen, the total ECRH power was only up to 4.3 MW with the upper limit of the energy uploaded into plasma estimated as 2 MJ, but later increased to 4 MJ.

Several Langmuir probes for measurements of periphery plasmas were integrated in the limiter. Additionally, several cameras for observation the limiter and wall have been installed, among them infrared cameras to measure temperature distribution on the limiter surface [14, 15]. For diagnostics of other in-vessel components

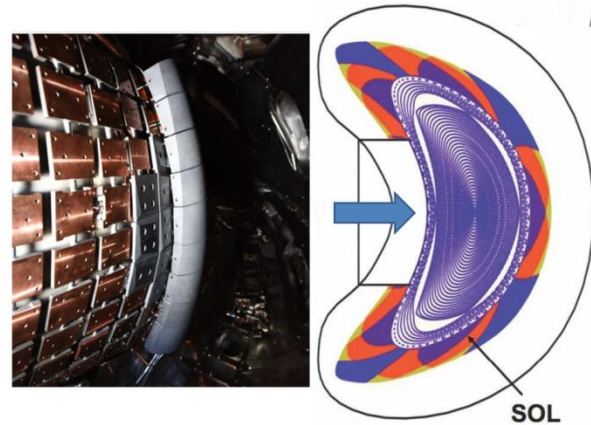


Fig. 1. The graphite limiter installed at the inner wall of torus in the bean-shaped cross-section (maximum of  $B$ ).

Also the layer which contacts with limiter is shown (courtesy to F. Effenberg)

and plasma edge, different types of camera were used, with a speed from 400 frames/s to 7 kframes/s and resolution from 1.3 to 1.0 Mpixel, respectively [14, 15].

Due to the ultra-fast cameras, filamentary structure of the edge plasma has been detected, usually at later phase of discharge accompanied by strong edge radiation (Fig. 2). These structures are aligned to the magnetic field lines, are extended toroidally in the whole volume, having in some cases a lifetime of a few milliseconds and revealing poloidal rotation [16].

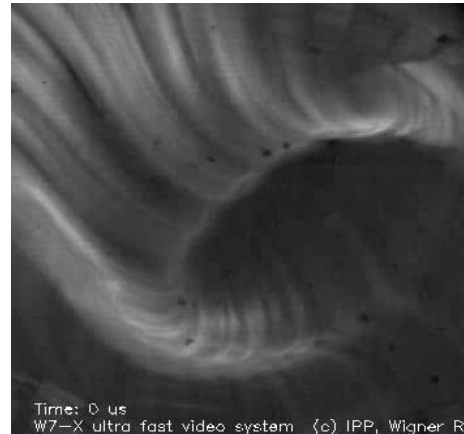


Fig. 2. Short exposure ( $\sim 20 \mu\text{s}$ ) of the periphery plasma with poloidally rotating filamentary structure

(by courtesy of M. Krychowiak)

For measurements of plasma parameters, more than 20 diagnostics have been applied [14,15]. In particular, Thomson scattering is applied for measurements of the electron density and temperature profiles ( $n_e$  and  $T_e$ , respectively), ECE diagnostics is used for  $T_e$  measurements, and imaging X-ray spectroscopy (XICS) yields both the electron and ion temperature profiles,  $T_e$  and  $T_i$ . Also interferometry is applied for getting the electron density averaged along the chord,  $\bar{n}_e = \int n_e dl/L$  with  $L \approx 1.3 \text{ m}$ . The diamagnetic loops are applied for measurement of energy stored in plasmas with an accuracy of 10 kJ (maximum value expected for diagnostics is about 5 MJ) and a time resolution of better than 1 ms. The Rogowski coils measured the net toroidal plasma current with an

accuracy of 100 A (generally, net toroidal currents are expected to be less 200 kA for the sum of bootstrap currents and ECCD).

In order to control the heating efficiency and prevent any damage of the wall and diagnostic tools due to non-absorbed RF power, W7-X is equipped by the protective ECRH diagnostics which contains five absolutely calibrated sniffer probes for the stray radiation [17] (shined through a power from gyrotrons).

## 2. EXPERIMENTAL RESULTS OF OP1.1

### 2.1. GENERAL ACHIEVEMENTS

Already during the first week of operation with helium plasmas, at line integrated density about  $2 \times 10^{19} \text{ m}^{-3}$ , electron and ion temperatures  $T_e \approx 1 \text{ keV}$  and  $T_i \leq 1 \text{ keV}$ , respectively, were accomplished. The duration of the early plasma discharges was limited to approximately 50 ms by radiative collapse of plasmas because of intensive outgassing from the wall and the limiter elements (initially, only baking of the chamber was performed). By series of short consecutive pulses of ECRH, the outgassing was reduced and duration of the pulses was significantly prolonged. Close to the end of first part of OP1.1, the following plasma parameters were achieved: for the discharge with 500 ms the temperatures  $T_e \approx 8 \text{ keV}$  and  $T_i \approx 2 \text{ keV}$  with the line-averaged density  $\bar{n}_e \approx 3 \times 10^{19} \text{ m}^{-3}$ . The typical plasma profiles for helium plasmas are shown in Fig. 3, where the radial profiles of  $n_e$ ,  $T_e$  and  $T_i$  in helium discharge with 4.0 MW ECRH are presented. Reproducibility of these results has been sufficiently high.

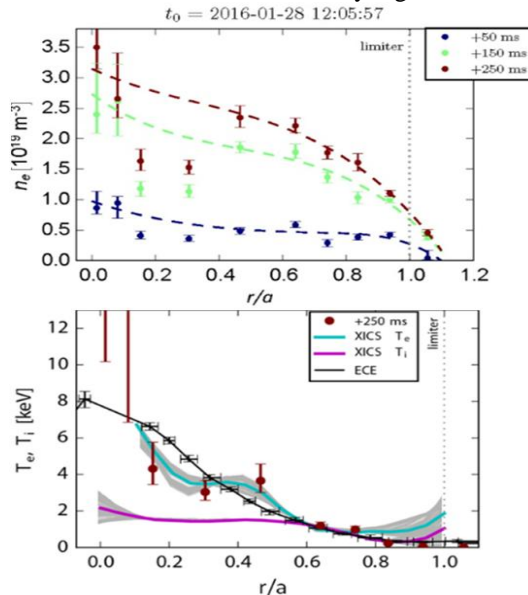


Fig. 3. Plasma density,  $n_e$  (top) and temperature,  $T_{e,i}$  (bottom) profiles of a helium plasma heated by 4 MW of ECRH (courtesy of M. Hirsch and E. Pasch)

However, the problem of outgassing and impurity accumulation was still open. Let us consider the typical example of the discharge with hydrogen, which was terminated because of radiative collapse. In Fig. 4, one can see that soon after the start-up with ECR heating power about 2 MW, the electron and ion temperatures reached the values about 7 keV and 1.2 keV, respectively, with line-averaged density about  $2 \times 10^{19} \text{ m}^{-3}$ . Find

that the time trace clearly shows the uncontrolled density ramping-up that leads to visible decreasing of  $T_e$  starting from 7th millisecond. Up to the moment when  $T_e$  becomes lower 1 keV, the unabsorbed ECRH power is kept negligible, but after rapidly increased. In this stage, a concentration of impurities becomes too high and the RF power absorbed by electrons is rapidly radiated without any thermalization, leading to further degradation of RF absorption with decreasing of electron temperature. This plasma state corresponds to the radiative collapse and ECRH is switched off. Please note that time behavior of  $T_i$  has an opposite to  $T_e$  tendency – growth together with density. This is an additional proof of good energy confinement for ions, which are heated only by collisions with electrons heated by ECRH, while the radiative cooling down becomes to be the main channel of energy losses for electrons.

In the 2nd part of OP1.1, for experiments with hydrogen plasmas, also the glue discharge technique for the wall cleaning becomes to be available making a further preventing the radiative collapse. This made a rapid progress: duration of the discharges was significantly extended being limited mainly by upper value of energy enabled to upload in the limiter. The main impurities observed in the plasma were oxygen and carbon, followed by traces of sulfur and chlorine [18] and surprisingly little indication for copper and iron.

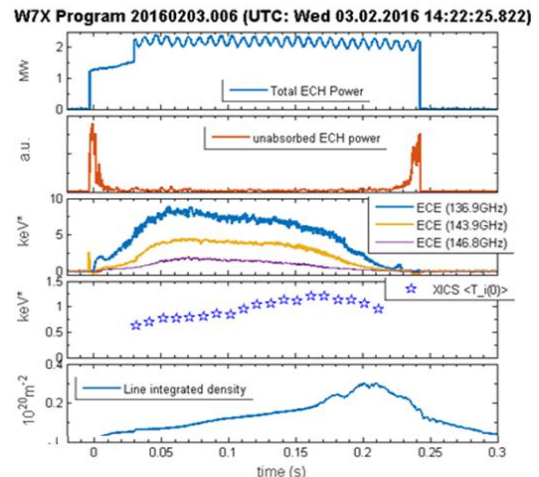


Fig. 4. Time-traces from 1st discharge with hydrogen. From up to down: ECRH power, non-absorbed stray radiation,  $T_e$ ,  $T_i$  and  $\int n_e dl$  (courtesy of A. Dinklage)

The typical achievements from the experiments with hydrogen plasmas are the following: for ECR heating with the power from 0.5 to 4 MW and the pulse length from 6 to 1 seconds, respectively, the temperatures  $T_e \approx 7 \dots 10 \text{ keV}$  and  $T_i \approx 1 \dots 2 \text{ keV}$  for density about  $(2 \dots 3) \times 10^{19} \text{ m}^{-3}$  have been obtained. One typical example is shown in Fig. 5, where the time traces together with the radial profiles of plasma parameters are shown for the discharge with total heating power 4.0 MW at the X2-mode and pulse duration 1.3 s. Please find that the density ramping-up was performed by gas puffing while an outgassing from the wall and impurity accumulation were practically negligible. The pulse length is limited only by the energy uploaded and no termination of the heating due to radiative collapse



required. One can see that plasma decay happens only after switching off the ECRH power.

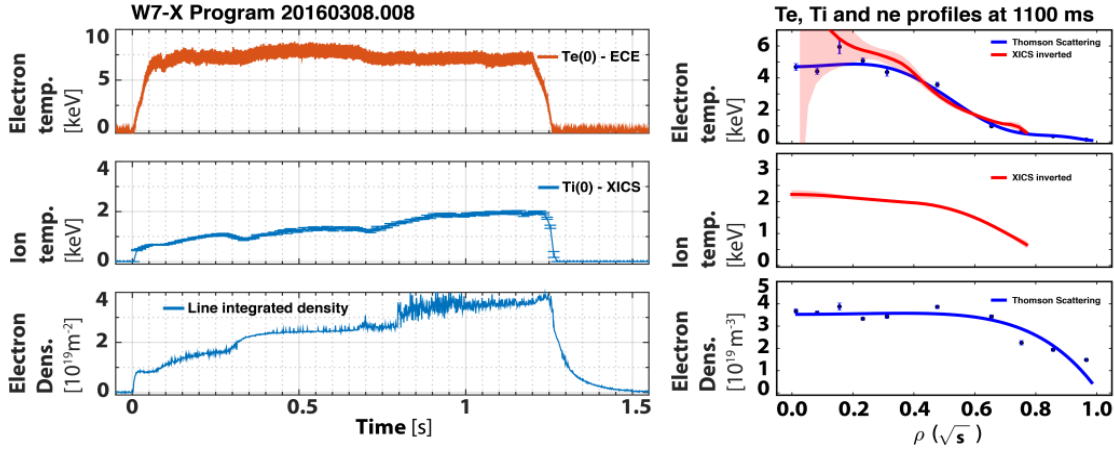


Fig. 5. Example of high performing plasmas achieved for 4.0 MW axial heating and 0.4 MJ stored energy. Left: time traces of  $T_e$ ,  $T_i$ , and  $\int n_e dl$ . Right: radial profiles of the same parameters (courtesy of N. Pablant)

## 2.2. CO- AND COUNTER CURRENT DRIVE

Electron cyclotron current drive (ECCD) is an important option in W7-X for compensating the bootstrap current which can make an impact to the island divertor [4,11,13]. In experiments, the current drive in both co- and counter with respect to the bootstrap current directions has been generated. It was performed by steering mirrors making an oblique launch of the RF beams with the toroidal angles  $\pm 10$  deg. The net plasma current contains the bootstrap current, ECCD and the reactive plasma response. While the characteristic times for establishing the bootstrap current and ECCD are of order of several collisional times (for present conditions this is about 1 ms), the characteristic time for an exponential decay of the inductive plasma response is much longer than others,  $L/R \approx 10$  s (pulse length is about 1 s). As consequence, the net plasma current measured by Rogowski coils is quite far from the steady state, especially for the case of co-current, when ECCD has the same direction as the bootstrap current, and the plasma response at the initial stage makes a screening up both of them. Nevertheless, for discharges with 2.0 MW heating and density about  $1 \times 10^{19} \text{ m}^{-3}$  the difference was clearly indicated: while the net current for counter injection was practically zero during the shot, in the case of co-injection the current demonstrated a mono-tonic growth from zero to approximately 1 kA. There was found also another specific feature of the short discharges with co-injection of high power RF beams: ECE channels which correspond to the central region show in the time-traces the short sawtooth-like crashes, indicating significant local disturbance of the  $\iota$ -profile [19].

## 2.3. CORE ELECTRON ROOT CONFINEMENT

The experiments for a specific stellarator regime of core “electron root” confinement (CERC) with strongly positive radial electric field,  $E_r$ , were performed [20]. This regime can be established if sufficiently high power of ECRH is applied making the electrons “overheated”,  $T_e \gg T_i$ . In this regime, the ambipolarity condition for neoclassical fluxes,  $\Gamma_e(E_r) = \sum Z_i \Gamma_i(E_r)$ ,

can be satisfied by establishing a highly positive radial electric field,  $E_r > 0$ , which is called usually as the “electron root” (in contrast to the “ion root”  $E_r < 0$ ). The neoclassical diffusion coefficient for electrons scales in this regime as  $\sqrt{\nu}$ , or, with explicit dependencies,  $D_{\sqrt{\nu}} \propto n_e^{1/2} T_e^{5/4} E_r^{-3/2}$  instead of unfavorable  $1/\nu$ -regime with  $D_{1/\nu} \propto \epsilon_{eff}^{3/2} n_e^{-1} T_e^{7/2}$ .

Fig. 6 (left) shows the plasma response to ECRH power steps 2.0, 0.6 and 1.3 MW. Switching the heating power down and up reveals response time scales in the plasma decay and build-up. One can note that  $T_e$  is in few times higher than  $T_i$  that indicates a collisional decoupling of ions from electrons. The most important, however, is that the speed of poloidal rotation due to  $E_r$  is significantly changing together with ECRH power: in the stage of 1.3 MW the speed is maximal, then, when the power is reduced to 0.6 MW, is close to zero, and increases with power again. Profiles of  $E_r(r)$  reconstructed the experimental data are in qualitative agreement with calculations from transport theory; see Fig. 6 (right). These findings confirm well the theoretical expectations from the neoclassical transport theory with respect to the low density regime of core “electron root” confinement also in W7-X [21].

## 2.4. ECRH WITH O-MODE 2ND HARMONICS

The standard ECRH scenario in W7-X at densities below  $1.2 \times 10^{20} \text{ m}^{-3}$  is the X2-mode which was used for most of the plasmas during OP1.1. At densities between  $1.2 \times 10^{20}$  and  $2.0 \times 10^{20} \text{ m}^{-3}$ , i.e. above the X2-cutoff, the O2-mode is required. Since, however, the maximal single-pass absorption of the O2-mode is estimated for W7-X about 70 %, a scenario with O2-heating requires the scheme with a multi-pass using reflecting surfaces inside the plasma-vessel. During OP1.1 the densities were lower than the X2 cut-off. However, unexpectedly high electron temperatures, which guarantee strong absorption of the RF beams, allowed performing the first O2-heating experiments [17].

At first the single-pass absorption was determined using a low power O2-beam in an otherwise X2-heated plasma. The absorption coefficient was measured com-

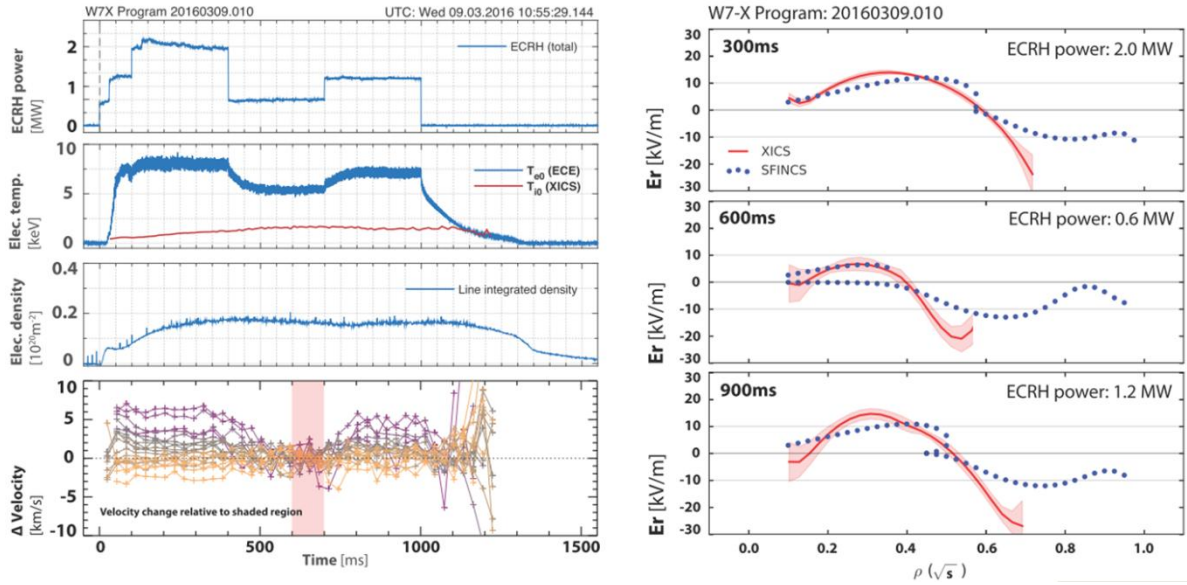


Fig. 6. CERC experiment, left: time-traces for ECRH power (X2-mode),  $T_e$ ,  $T_i$ ,  $\bar{n}_e$  and speed of poloidal plasma rotation due to  $E_r$  (Doppler shift measurements from the X-ray imaging crystal spectrometer). Right: profiles of the  $E_r$ , experimental (red lines) and theoretical (blue points), shown for three time-points corresponding to the different regimes of confinement (courtesy of N. Pablant)

paring the ECA signal with and without plasma. Consistently with ray-tracing calculations, single-pass absorption about 70 % was achieved for  $T_e$  exceeding 5 keV. In a second step the plasma purely by O2-mode heated was established.

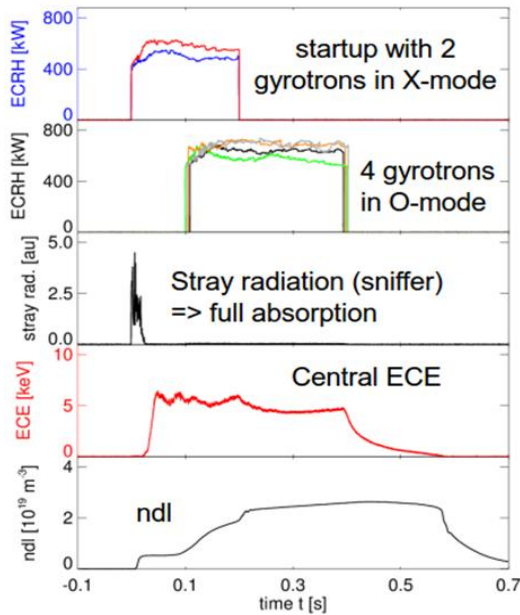


Fig. 7. Time-traces for O2-scenario

Fig 7 illustrates the multi-pass absorption scheme in W7-X and shows the discharge parameters for a case where the heating was changed from X2 to O2. The plasma start-up was performed using two gyrotrons with X2-mode. After reaching central  $T_e$  of 5 keV, RF beams from four gyrotrons in O2-mode were added. Finally, the X2-beams were switched off and the discharge was sustained purely by O2-heating with stable  $T_e$  about 4 keV. The line-averaged density in this experiment did not exceed  $3 \times 10^{19} \text{m}^{-3}$  being much lower of optimal for operation with O2-mode. Nevertheless, an overall

absorption of about 95 % was obtained. This is the 1st successful experiment with pure O<sub>2</sub> heating.

## CONCLUSIONS

OP1.1 started using helium plasmas and after quick progress in experiments, from February, 3rd, 2016, with inauguration ceremony in presence of the German Federal Chancellor Dr. Angela Merkel, an operation with hydrogen plasmas started. The OP1.1 campaign was completed on March, 10th, 2016.

Overall, with totally about 2200 pulses, 940 discharge programs were performed. 92 of them were technical tests, 446 were dedicated to the basic plasma performance (e.g. plasma-vessel conditioning), and 402 were dedicated to physics studies. This allowed for a first assessment of the confinement properties of the magnetic field configuration, the investigation of transport at the plasma boundary, and many other programs for different ECRH scenarios.

The start of operation with plasmas was surprisingly successful. Already during the first week of work with helium plasmas, electron temperatures of 1 keV were reached. The duration of the early discharges was limited due to accumulation of impurities and radiative collapse to approximately 50 ms. After applying short consecutive pulses of ECRH, the conditioning of the plasma vessel was improved that made possible to prolong the discharge duration to (depending from power) from hundreds milliseconds to several seconds.

The initial hydrogen plasmas of W7-X have proven to be robust and well controllable if a sufficient conditioning of the metal wall and the inboard limiters was performed. There was found that glow discharge wall conditioning is most effective, though conditioning shots with ECRH also made significant improvement. Apart from the upper limit of the energy uploaded in plasmas defined from safety of the limiter, the main pulse length limitation is due to the radiation collapse. However, after glow discharge conditioning and ECRH

wall conditioning pulses, stable and reproducible discharges could be achieved from low ECRH power (0.6 MW with duration up to 6 s) to higher power (4.3 MW with duration of 1 s). Better performance is expected after the island divertor has been installed and the majority of the wall is covered with graphite tiles.

A strong evidence for the specific stellarator regime of central "electron-root" confinement was found, with peaked  $T_e$  profiles and a strongly positive radial electric field in the core region. The experiments with ECCD generation in both co- and counter directions with respect to the bootstrap current were also successful. There was successfully performed first in the world the ECRH scenario with O2-mode alone with stable hot plasmas. Important to mention also that the main results are in satisfactory agreement with the theory predictions.

The success of the first experimental campaign exceeded the initial expectations. Originally, the aim was to perform an integral commissioning of the W7-X operation, including ECRH and the first set of plasma diagnostics (more than 20). However, swift progress enabled many in-depth physics studies. Not least, this was made possible by the extremely reliable operation and interplay between the various technical systems of W7-X, in particular the cryoplant, the superconducting magnet system, the device control, and the ECRH plant.

More than half of the physics program involved collaborations: in about 40% of the experiments, the proposals were conducted in the frame of European collaborations and in 24% with partners from the US. The largest part of the experiments, however, involved all parties which can be seen as a successful implementation of the one-team-approach.

*This work has been carried out within the frame-work of the EUROfusion Consortium and has received funding from the Euratom research and training programme 2014-2018 under grant agreement No 633053. The views and opinions expressed herein do not necessarily reflect those of the European Commission.*

## REFERENCES

1. T. Klinger and the Wendelstein 7-X Team // *43rd EPS Conf. on Plasma Physics*, July 4-8, 2016, Leuven, Belgium; EV.001.
2. L. Wegener et al. // *IEEE Trans. Appl. Superconduct.* 2012, v. 22, № 3, p. 4201004.
3. G. Grieger et al. // *Fusion Technol.* 1992, v. 21, p. 1767.
4. G. Grieger et al. // *Phys. Fluids. B.* 1992, v. 4, p. 2081.
5. J. Nührenberg, R. Zille // *Phys. Lett. A.* 1986, v.114, p. 129.
6. J. Nührenberg, R. Zille // *Phys. Lett. A.* 1988, v. 129, p. 113
7. J. Geiger et al. // *Plasma Phys. Control. Fusion.* 2015, v. 57, p. 014004.
8. M. Hirsch et al. // *Plasma Phys. Control. Fusion.* 2008, v. 50, p. 053001.
9. F. Warmer et al. // *Plasma Phys. Control. Fusion.* 2016, v. 58, p. 074006.
10. J. Nührenberg, E. Strumberger // *Contrib. Plasma Phys.* 1992, v. 32, № 3/4, p. 204.
11. V. Erckmann et al. // *Fusion Sci. Technol.* 2007, v. 52, p. 291.
12. J. Boscary et al. // *Fusion Eng. Des.* 2011, v. 86, p. 572.
13. T.S. Pedersen et al. // *Nucl. Fusion.* 2015, v. 55, p. 126001.
14. R. König et al. // *J. Instr.* 2015, v. 10, p. P10002.
15. M. Krychowiak et al. // *Rev. Sci. Instr.* 2016, v. 87, p. 11D304.
16. G. Kocsis et al. // *43rd EPS Conf. on Plasma Physics*. July 4-8, 2016, Leuven, Belgium; P4.003.
17. S. Marsen et al. // *26th IAEA Fusion Energy Conf.* Kyoto. 17-22 October 2016, EX/P5-13.
18. T. Wauters et al. // *43rd EPS Conf. on Plasma Physics*, July 4-8, 2016, Leuven, Belgium; P4.047.
19. R.C. Wolf et al. // *26th IAEA Fusion Energy Conf.*, Kyoto, 17-22 Oct. 2016, OV/3.1.
20. A. Dinklage et al. // *43rd EPS Conf. on Plasma Physics*, July 4-8, 2016, Leuven, Belgium; O2.107.
21. M. Yokoyama et al. // *Nucl. Fusion.* 2007, v. 47, p. 1213.

*Article received 22.11.16*

## ОСНОВНЫЕ РЕЗУЛЬТАТЫ ПЕРВОЙ ЭКСПЕРИМЕНТАЛЬНОЙ КАМПАНИИ НА СТЕЛЛАРАТОРЕ W7-X

*Н.Б. Маруценко и др.*

Представлены итоги первой экспериментальной кампании (OP1.1) на стеллараторе W7-X. Вкратце описана специфика эксперимента, методов нагрева и основных диагностик. Параметры плазмы и удержание, полученные в экспериментах, превысили ожидаемые:  $T_e > 8$  кэВ и  $T_i > 2$  кэВ при  $\bar{n}_e \approx 3 \times 10^{19} \text{ м}^{-3}$ , что соответствует  $\beta_0 \approx 2.5$  %. Результаты по ЭЦР-нагреву на X2-моду, а также по токам увлечения согласуются с теорией. Впервые был успешно реализован сценарий нагрева на O2-моду. Был также получен специфический для стеллараторов режим "электронного корня" удержания.

## ОСНОВНІ РЕЗУЛЬТАТИ ПЕРШОЇ ЕКСПЕРИМЕНТАЛЬНОЇ КАМПАНІЇ НА СТЕЛАРАТОРІ W7-X

*М.Б. Маруценко та інші.*

Представлені підсумки першої експериментальної кампанії (OP1.1) на стеллараторі W7-X. Коротко описана специфіка експерименту, методів нагріву та діагностики. Параметри плазми та удержання, отримані в експериментах, перевищили очікувані:  $T_e > 8$  кеВ та  $T_i > 2$  кеВ при  $\bar{n}_e \approx 3 \times 10^{19} \text{ м}^{-3}$ , що відповідає  $\beta_0 \approx 2.5$  %. Результати по ЕЦР-нагріву на X2-моді, а також по струмам захоплення відповідають теорії. Вперше був успішно реалізований сценарій нагріву на O2-моді. Був також успішно реалізований специфічний для стеллараторів режим "електронного кореня" утримання.